JACS
JOURNAL OF THE AMERICAN CHEMICAL SOCIETY
Communication
pubs.acs.org/JACS

Subsecond and in Situ Chemical Speciation of Pt/Al_2O_3 during Oxidation–Reduction Cycles Monitored by High-Energy Resolution Off-Resonant X-ray Spectroscopy

Jakub Szlachetko,*[,†,‡,⊥] Davide Ferri,[†] Valentina Marchionni,[†] Anastasios Kambolis,[†] Olga V. Safonova,[†] Christopher J. Milne,[†] Oliver Kröcher,[†,§] Maarten Nachtegaal,[†] and Jacinto Sá*[,†,⊥]

[†]Paul Scherrer Institut, CH-5232 Villigen PSI, Switzerland

[‡]Institute of Physics, Jan Kochanowski University, P-25-406 Kielce, Poland

[§]École Polytechnique Fédérale de Lausanne, CH-1015 Lausanne, Switzerland

Supporting Information

ABSTRACT: We report an in situ time-resolved high-energy resolution off-resonant spectroscopy study with subsecond resolution providing insight into the oxidation and reduction steps of a Pt catalyst during CO oxidation. The study shows that the slow oxidation step is composed of two characteristic stages, namely, dissociative adsorption of oxygen followed by partial oxidation of Pt subsurface. By comparing the experimental spectra with theoretical calculations, we found that the intermediate chemisorbed O on Pt is adsorbed on atop position, which suggests surface poisoning by CO or surface reconstruction.

Platinum-based catalysts are indisputably the most important class of heterogeneous catalysts used by the chemical industry. They are used in a plethora of chemical processes from the production of fertilizers and plastics to pharmaceuticals. Environmental protection also exploits Pt-based catalysts. Furthermore Pt catalysts are a key component of proton exchange membrane fuel cells (PEMFC),[1] which are seen as a promising technology for a renewable-energy infrastructure. An unresolved prerequisite is the development of cost-effective electrocatalysts, in particular for the oxygen reduction reaction (ORR). Platinum-based catalysts exhibit the best electrocatalytic performance;[2] thus, significant effort has been made to understand the intricacies of the process.

Conventional spectroscopic techniques used to detect surface composition during a catalytic reaction are often unable to pinpoint the metal electronic states because they either are not surface specific and/or cannot be carried out under working conditions. X-ray absorption spectroscopy (XAS) is able to identify the chemical states under working conditions due to the high penetration of X-rays.[3] With the advent of high resolution XAS (HR-XAS), the determination of the unoccupied Pt *5d* states has become accessible by probing the Pt L_3-edge transition, which is sensitive to metal oxidation state, as well as to the presence of adsorbed species.[4] Currently, the major limitation of HR-XAS is its time resolution, which is of the order of tenths of seconds for ideal samples with high metal concentration, such as single crystals, and measured at high photon flux sources. The limitation arises from the fact that XAS measurements require scanning of the incoming energy, which is limited to the speed at which the monochromator can be moved. This makes it difficult to follow a catalytic process in real time.

Previous HR-XAS studies of ORR were carried out in a stepwise mode; i.e., the potential was adjusted to a predetermined value, and the spectra were collected until statistically relevant signals were measured, often taking at least tenths of minutes, before moving to the next potential. Ideally, the experiments should be carried out in continuous mode in which potential variation and data collection are carried out synchronously and uninterruptedly, enabling the identification of metastable regimes and intermediate species.[5] High-energy resolution off-resonant spectroscopy (HEROS) can provide element-specific information about the unoccupied density of states.[6] Because of the scanning free arrangement, the HEROS spectra can be recorded with very high time resolution (only depending on sample concentration and photon flux), while maintaining an energy resolution independent of the initial lifetime broadening.[7] Moreover, HEROS spectra are not affected by the self-absorption process, thus making it a powerful technique to identify and quantify the desired structural changes during a catalytic reaction.

In this work, we demonstrate that chemical speciation can be obtained on a Pt/Al_2O_3 catalyst during reaction without sacrificing time and spectral resolution. In situ time-resolved HEROS spectra were recorded continuously around the L_3 absorption edge (10 eV detuning) and the $L\alpha_1$ X-ray emission with an acquisition time of 500 ms/spectrum using the von Hamos-type spectrometer of the at SuperXAS beamline (Swiss Light Source).[7] In order to increase the signal-to-noise ratio, 120 cycles were performed and averaged, which equals to 2 h total acquisition time.

Before discussing the spectra, we would like to emphasize that the Pt L_3-edge HEROS whiteline reflects the unoccupied *5d* state population,[8] and the HEROS edge position (high energy side of the spectrum) is a direct measurement of the element absorption edge position (Fermi level), which can be retrieved through the energy conservation formula:

$$E_{\text{edge}} = E_{\text{beam}} + E_{f\rightarrow i} - E_{\text{HEROS}}$$

Received: October 10, 2013
Published: December 9, 2013

   dx.doi.org/10.1021/ja410146c | J. Am. Chem. Soc. 2013, 135, 19071–19074

where E_{edge} is the energy of the absorption edge (inflection point), E_{beam} is the energy of the incoming beam (constant, in present experiment E_{beam} = 11550 eV), and $E_{f\rightarrow i}$ is the energy of transition from the final to the initial state, in this case $3d \rightarrow 2p$ transition (constant, $E_{L\alpha 1}$ = 9442 eV). E_{HEROS} stands for the inflection point position on the high energy side of the HEROS spectrum (around 9432 eV). The equation clearly demonstrates that the spectral shift to higher energy in the HEROS spectrum is caused by the energy lowering of the corresponding absorption edge; i.e., the energy shifts of HEROS are opposite to those recorded with XAS techniques.

The temporal evolution of the averaged HEROS spectra recorded on 1.3 wt % Pt/Al_2O_3 during a full cycle of reduction in 4 vol % CO (5−35 s) and oxidation in 4 vol % O_2 (0−5 s, and 35−60s) at 300 °C is plotted in Figure 1. The 2D map is

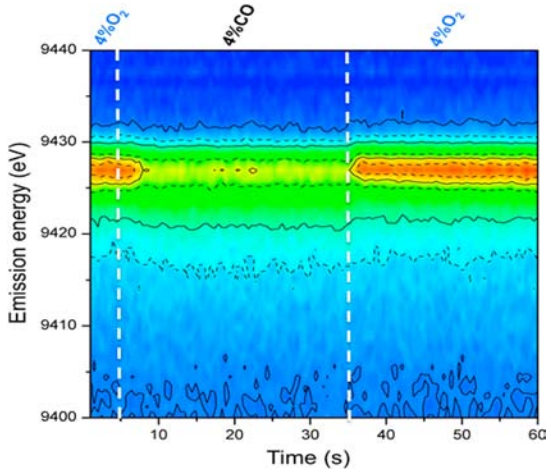

Figure 1. Temporal evolution of the HEROS spectra during CO/O_2 switches at 300 °C on 1.3 wt % Pt/Al_2O_3.

dominated by the whiteline region (9425−9428 eV). The whiteline intensity and position repeatedly change throughout the reduction and oxidation steps, thus reflecting the reversible variation of the *5d* density of empty states. To better evaluate the changes observed in the HEROS data, the temporal profiles of the signals at 9426 and 9427 eV emission energy are plotted in Figure 2. Several considerations can be made from analysis of the evolution of the signals. First, both oxidation and reduction

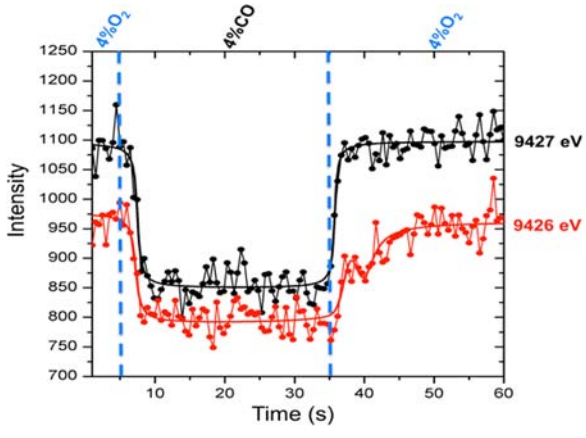

Figure 2. Temporal evolution of the HEROS signals at 9426 and 9427 eV (whiteline region) during CO/O_2 switches.

final states are achieved within ca. 5 s. The final state of reduction is achieved slightly faster than oxidation and does not show evidence for an intermediate step because the profiles of both emission energies are characterized by a continuous and smooth decrease of whiteline intensity. Contrarily, in the oxidation step the 9426 eV emission energy exhibits an intense peak centered at 39 s before reaching a plateau 15 s after the switch (Figure S2, Supporting Information (SI)). The peak suggests the formation of a metastable intermediate state. The HEROS spectra retrieved from Figure 1 at time 31 s (reduced state), 39 s (oxidation intermediate state), and 58 s (oxidized state) are plotted in Figure 3 (top).

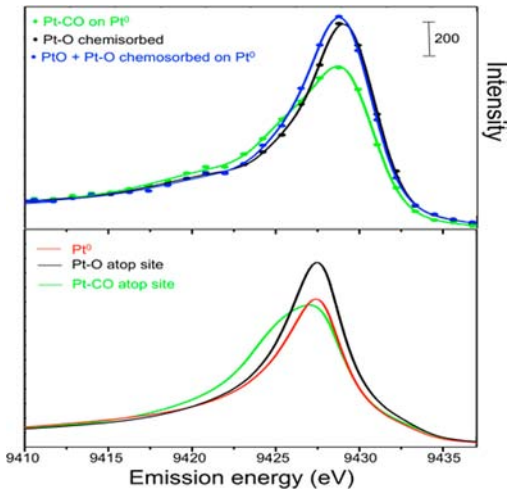

Figure 3. (top) HEROS spectra extracted in the regions of interest during CO/O_2 switches, namely, after 31 s (green), 37 s (black), and 58 s (blue). (bottom) Theoretical HEROS spectra of the species of interest.

The spectrum after platinum reduction in CO (green) is slightly broader and has a smaller whiteline than the one expected for Pt^0. This suggests the presence of a second spectral component beside metallic platinum. Theoretical calculations performed with FEFF9[9] assigned the second component to CO chemisorbed on Pt in atop position (most energetically favored adsorption site of CO on Pt).[10] As in the experimental spectrum, this species exhibits a broader signal on the low energy side with slightly lower whiteline intensity (Figure 3 bottom, green).[11]

The spectrum collected on the plateau during oxidation (blue) shows significantly higher whiteline intensity and an edge shift to higher energy with respect to the spectrum of metallic Pt collected in the CO pulse, which hints to an increase of Pt oxidation state, according to the energy conservation formula. The spectrum of the Pt intermediate state (Figure 3 top, black), extracted at the peak in the profile of the signal at 9426 eV, i.e., at t = 39 s, differs appreciably from the spectrum of the final oxidation state. The spectrum possesses an intense whiteline, which is shifted to higher energy with respect to the spectrum of metallic platinum. The simple fact that intermediate states can be observed demonstrates HEROS enhanced capabilities in terms of temporal resolution and high chemical sensitivity. Theoretical calculations imply that the spectrum is associated with chemisorbed O, more specifically with chemisorbed O on Pt in atop position (Figure 3 bottom, black). The adsorbate−surface bonding leads to an electron transfer from the Pt site to the activated oxygen atom that is

dx.doi.org/10.1021/ja410146c | J. Am. Chem. Soc. 2013, 135, 19071−19074

reflected in the increase of the unoccupied density of states of Pt.[12] The small shift suggests that O-bonding is weaker than CO and insufficient to induce a change of Pt oxidation state. The result is significant, because the preferred adsorption site for dissociated oxygen on Pt is the 3-fold site (hollow site).[12] The result can be rationalized either in terms of surface poisoning by CO[13] or surface reconstruction. The former blocks access of the activated oxygen to its energetically favored site until CO has been cleared upon oxidation. The latter generates different Pt sites where activated oxygen can adsorb. Finally, when comparing the Pt intermediate state with the spectrum recorded on the oxidation plateau, we note that the shift and the whiteline intensity are not characteristic of a fully oxidized structure. Instead the spectrum is composed of partially oxidized surface with a strong contribution from chemisorbed O, and a small contribution from metallic platinum, most likely in the core of the Pt nanoparticle.[14,15]

To confirm the proposed hypothesis of O intermediate species adsorbed on atop position, we carried out an identical experiment in which CO was replaced by H_2 as the reducing agent (Figure S3 (SI)). As with the CO/O_2 cycles, the final state of reduction and oxidation was obtained within a few seconds. Horizontal cuts at 9427 and 9428 eV emission energy (Figure S3 (SI)) show that oxidation and reduction steps are faster when H_2/O_2 is used instead of CO/O_2. Similarly to the CO/O_2 case, an intermediate species was detected during the oxidation.

The HEROS spectrum of Pt retrieved from Figure S4 (SI) recorded after 32 s during reduction was fitted to metallic platinum (Pt^0) exclusively (Figure 4). No evidence was found

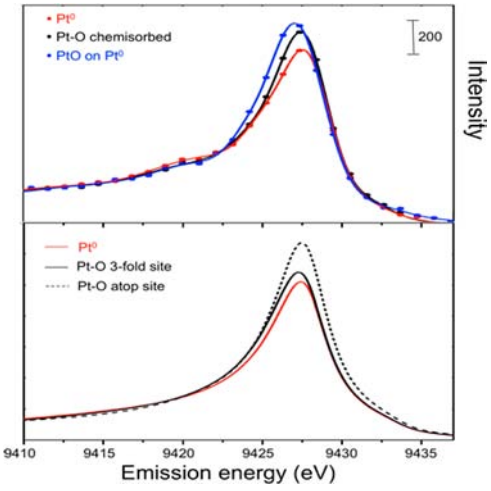

Figure 4. (top) HEROS spectra extracted in the regions of interest during H_2/O_2 switches, namely, after 32 s (red), 38 s (black), and 58 s (blue). (bottom) Theoretical HEROS spectra of species of interest.

for the presence of activated hydrogen on the surface. This is not surprising since H_2 oxidizes at much lower temperatures than our reaction temperature (300 °C).[16] According to a previous assignment, activated H_2 causes a minor shift of the absorption edge to higher energy (HEROS lower energy).[17]

The final state in the oxidation step (spectrum after 58 s) is consistent with the formation of PtO_x (Pt^{2+}) but with a small fraction of metallic platinum suggesting partial oxidation of the metal particle. The spectrum corresponding to the intermediate state (38 s) has a slightly more intense whiteline than the spectrum of metallic platinum, but importantly it is not shifted in energy (Figure S5 (SI)). Theoretical calculations suggest that in this case chemisorbed O occupies the preferred 3-fold site (Figure 4, bottom). The result confirms the sensitivity of HEROS to different O adsorption geometries and our hypothesis that surface poisoning by CO forces the oxygen to chemisorb on Pt in atop position. For comparison, the HEROS spectra for final reduction and oxidation states during the CO/O_2 and H_2/O_2 cycles (Figure S6 (SI)) demonstrate that the Pt electronic final states differ in the two experiments. In contrast to reduction by H_2, the CO reduction results in CO-Pt species with CO adsorbed in atop position, clearly depicted in the HEROS spectrum by the broadening of the *5d* states distribution. The final oxidation state of CO/O_2 cycles shows higher Pt *5d* unoccupied density of states with simultaneous shift of the edge position. Surface poisoning is the most likely reason for the difference, especially during oxidation, since before Pt oxidation the chemisorbed CO must be removed, which is achieved via CO oxidation to CO_2.

In conclusion, we demonstrated that HEROS is able to perform chemical speciation with subsecond time resolution, which opens exciting opportunities to follow catalysis in real time. We showed that using HEROS we could obtain unprecedented insight into the elementary reaction steps of CO oxidations/reductions. Moreover, we demonstrate that the oxidation−reduction rates depend on gas feed composition and identified the formation of reaction intermediates (chemisorbed Pt−O), and final states including chemisorbed Pt−CO species. The adsorption geometry of chemisorbed oxygen depends on the surface coverage of CO, which can induce surface poisoning or reconstruction. Since the HEROS spectra are collected in a single shot, the time resolution can be further improved since it depends only on the number of incoming photons and element concentration, which makes it particularly suited for experiments at the X-ray free electron lasers.

■ ASSOCIATED CONTENT

Supporting Information

Experimental details, data concerning H_2/O_2 cycling and time-resolved spectra. This information is available free of charge via the Internet at http://pubs.acs.org.

■ AUTHOR INFORMATION

Corresponding Author

jakub.szlachetko@psi.ch; jacinto.sa@psi.ch

Author Contributions

⊥J. Szlachetko and J. Sá contributed equally.

Notes

The authors declare no competing financial interest.

■ ACKNOWLEDGMENTS

The authors would like to acknowledge the Swiss Light Source (SLS) for access to the SuperXAS beam line. The authors acknowledge financial support from the PSI, the SNF (Project No. 200021_138068), and CCMX.

■ REFERENCES

(1) For example: (a) Tian, N.; Zhou, Z.-Y.; Sun, S.-G.; Ding, Y.; Wang, Z. L. *Science* **2007**, *316*, 732−735.

(2) (a) Strasser, P.; Koh, S.; Anniyev, T.; Greeley, J.; More, K.; Yu, C.; Liu, Z.; Kaya, S.; Nordlund, D.; Ogasawara, H.; Toney, M. F.; Nilson, A. *Nat. Chem.* **2010**, *2*, 454−460. (b) Zhang, J. L.; Vukmirovic, M. B.; Mavrikakis, M.; Adzic, R. R. *Angew. Chem., Int. Ed.* **2005**, *44*, 2132−2135. (c) Greeley, J.; Stephens, I. E. L.; Bondarenko, A. S.;

Johansson, T. P.; Hansen, H. A.; Jaramillo, T. F.; Rossmeisl, J.; Chrokendorff, I.; Nørskov, J. K. *Nat. Chem.* **2009**, *1*, 552−556. (d) Stamenkovic, V. R.; Fowler, B.; Mun, B. S.; Wang, G. F.; Ross, P. N.; Lucas, C. A.; Markovic, N. M. *Science* **2007**, *315*, 493−497.

(3) For example: (a) Tada, M.; Murata, S.; Asakoka, T.; Hiroshima, K.; Okumura, K.; Tanida, H.; Tanida, H.; Uruga, T.; Nakanishi, H.; Matsumoto, S.-i.; Inada, Y.; Nomura, M.; Iwasawa, Y. *Angew. Chem., Int. Ed.* **2007**, *46*, 4310−4315. (b) Zhang, J.; Sasaki, K.; Sutter, E.; Adzic, R. R. *Science* **2007**, *315*, 220−222. (c) Bordiga, S.; Groppo, E.; Agostini, G.; van Bokhoven, J. A.; Lamberti, C. *Chem. Rev.* **2013**, *113*, 1736−1850.

(4) For example: (a) Friebel, D.; Miller, D. J.; Nordlund, D.; Ogasawara, H.; Nilsson, A. *Angew. Chem.* **2011**, *123*, 10372−10374. (b) Friebel, D.; Viswanathan, V.; Miller, D. J.; Anniyev, T.; Ogasawara, H.; Larsen, A. H.; O'Grady, C. P.; Nørskov, J. K.; Nilsson, A. *J. Am. Chem. Soc.* **2012**, *134*, 9664−9671. (c) Singh, J.; Lamberti, C.; van Bokhoven, J. A. *Chem. Soc. Rev.* **2010**, *39*, 4754−4766.

(5) Bauer, P. R.; Bonnefont, A.; Krischer, K. *ChemPhysChem* **2010**, *11*, 3002−3010.

(6) Szlachetko, J.; Nachtegaal, M.; Sá, J.; Dousse, J.-C.; Hoszowska, J.; Kleymenov, E.; Janousch, M.; Safonova, O. V.; van Bokhoven, J. A *Chem. Commun.* **2012**, *48*, 10898−10900.

(7) Szlachetko, J.; Nachetgaal, M.; de Boni, E.; Safonova, O.; Sá, J.; Smolentsev, G.; Szlachetko, M.; van Bokhoven, J. A.; Dousse, J.-C.; Hoszowska, J.; Kayser, Y.; Jagodzinski, P.; Bergamaschi, A.; Schmid, B.; David, C.; Lücke, A. *Rev. Sci. Instrum.* **2012**, *83*, 103105.

(8) (a) Horsley, J. A. *J. Chem. Phys.* **1982**, *76*, 1451−1458. (b) Mansour, A. N.; Cook, J. W.; Sayers, D. E. *J. Phys. Chem.* **1984**, *88*, 2330−2334. (c) de Groot, F. M. F.; Krisch, M. H.; Vogel, J. *Phys. Rev. B: Condens. Matter* **2002**, *66*, 195112. (d) Safonova, O. V.; Tromp, M.; van Bokhoven, J. A.; de Groot, F. M. F.; Evans, J.; Glatzel, P. *J. Phys. Chem. B* **2006**, *110*, 16162−16164.

(9) (a) Ankudinov, A. L.; Ravel, B.; Rehr, J. J.; Conradson, S. D. *Phys. Rev B* **1998**, *58*, 7565. (b) Ankudinov, A. L.; Rehr, J. J.; Low, J.; Bare, S. R. *Phys. Rev. Lett.* **2001**, *86*, 1642.

(10) (a) Liu, Z.-P.; Hu, P. *Top. Catal.* **2004**, *28*, 71−78. (b) Zhang, C. J.; Hu, P. *J. Am. Chem. Soc.* **2001**, *123*, 1166−1172.

(11) Sá, J.; Szlachetko, J.; Sikora, M.; Kavčič, M.; Safonova, O. V.; Nachtegaal, M. *Nanoscale* **2013**, *5*, 8462−8465.

(12) Vicente, B. C.; Nelson, R. C.; Singh, J.; Scott, S. L.; van Bokhoven, J. A. *Catal. Today* **2011**, *160*, 137−143.

(13) Trimm, D. L.; Önsan, Z. I. *Catal. Rev.* **2001**, *43*, 31−84. (b) Jacobson, M. Z.; Colella, W. G.; Golden, D. M. *Science* **2005**, *308*, 1901−1905.

(14) Merte, L. R.; Behafarid, F.; Miller, J.; Friebel, D.; Cho, S.; Mbuga, F.; Sokaras, D.; Alonso-Mori, R.; Weng, T.-C.; Nordlund, D.; Nilsson, A.; Cuenya, B. R. *ACS Catal.* **2012**, *2*, 2371−2376.

(15) Friebel, D.; Miller, D. J.; O'Grady, C. P.; Anniyev, T.; Bargar, J.; Bergmann, U.; Ogasawara, H.; Wikfeldt, K. T.; Pettersson, L. G. M.; Nilsson, A. *Phys. Chem. Chem. Phys.* **2011**, *13*, 262−266.

(16) For example: Pedrero, C.; Waku, T.; Iglesia, E. *J. Catal.* **2005**, *233*, 242−255.

(17) Manyar, H. G.; Morgan, R.; Morgan, K.; Yang, B.; Hu, P.; Szlachetko, J.; Sá, J.; Hardacre, C. *Catal. Sci. Technol.* **2013**, *3*, 1497−1500.